

A change in boundary conditions induces a discontinuity of tissue flow in chicken embryos and the formation of the cephalic fold*

V. Fleury^a

Laboratoire Matière et Systèmes Complexes, Université Paris Diderot, 10 rue Alice Domon et Léonie Duquet, 75013 Paris France

Received 26 August 2010 and Received in final form 15 March 2011

Published online: 28 July 2011 – © EDP Sciences / Società Italiana di Fisica / Springer-Verlag 2011

Abstract. The morphogenesis of vertebrate body parts remains an open question. It is not clear whether the existence of different structures, such as a head, can be addressed by fundamental laws of tissue movement and deformation, or whether they are only a sequence of stop-and-go genetic instructions. I have filmed by time-lapse microscopy the formation of the presumptive head territory in chicken embryos. I show that the early lateral evagination of the eye cups and of the mesencephalic plate is a consequence of a sudden change in boundary conditions of the initial cell flow occurring in these embryos. Due to tissue flow, and collision of the two halves of the embryo, the tissue sheet movement is first dipolar, and next quadrupolar. *In vivo* air puff tonometry reveals a simple visco-elastic behaviour of the living material. The jump from a dipolar to a quadrupolar flow changes the topology of the early morphogenetic field which is observed towards a complex vortex winding with a trail (the eye cups and brain folds). The hydrodynamical model accounts for the discontinuity of the vector field at the moment of collision of the left and right halves of the embryo, at a quantitative level. This suggests a possible mechanism for the morphogenesis of the head of amniotes, as compared to cephalochordates and anamniotes.

Introduction

It has long been known that mechanical forces play a role in embryo development [1–3]. Mechanics participates in animal development from the cellular stage (for example in the process of cortical rotation [4]), up to morphogenesis and tissue organization in the adult (for example in cartilage formation [5]). More recently, the coupling between mechanical issues, and genetic expressions has been put forward repeatedly [6–9]. In parallel, technical progress in embryo imaging has allowed one to reconstruct displacement fields during embryo development, and correlate them to the possible pattern of cell traction forces [10, 11], and to the general dynamics of tissue expansion [12].

We address in this article the morphogenetic movements observed in chicken embryos, in the rostral part of the body (the presumptive head). The purpose is to analyze and understand the physical features of the field of displacements during early morphogenesis of the amniote head. The study is made in the chicken model, and will deal with the second day of development in this animal model. Whether the results can be extrapolated to other vertebrates is discussed in conclusion.

Vertebrates belong to the *phylum* of chordates [13], the chordates subdivide into cephalochordates and vertebrates. Cephalochordates are non-craniates, their head is just an oral tube-like opening. Craniates (the ones with a true head) form their head from a neural tube. The formation of the neural tube is one step in a complex sequence of morphogenetic movements. These movements start off from a round or discoidal mass of cells, comprising about thirty thousand cells in chicken [14]. At the moment which interests us, these cells form a sheet called generally epiblast. At this early developmental stage, large convergent movements occur towards the median axis, which transform the epiblast into a recognizable vertebrate. During a first phase of these movements, one fraction (about one half) of the epiblast invaginates to create the so-called mesoderm [15]. After this stage, the embryo is still flat and “formless”, but stratified, with ectoderm on top, mesoderm in the middle layer, and endoderm underneath.

Then, as the movements continue, the embryo surface starts to fold, and in about 36 hours (in the chicken), a recognizable vertebrate, with dorsal axis, eye cups, pelvic winding, segmented precursors of vertebrae, etc. is formed. The head (esp. skull, eyes and nose) form from a pair of folds called neural folds, which form a distinct tube located dorsally (the mouth and jaw are ventral structures and will not be discussed here). In most animals, including chicken, this tube forms by rolling up of the ectoderm and it is called neural tube [16]. In fish, the formation of the tube

* Supplementary material in the form of a .gif file available from the Journal web page at

<http://dx.doi.org/10.1140/epje/i2011-11073-0>

^a e-mail: vincent.fleury@univ-paris-diderot.fr

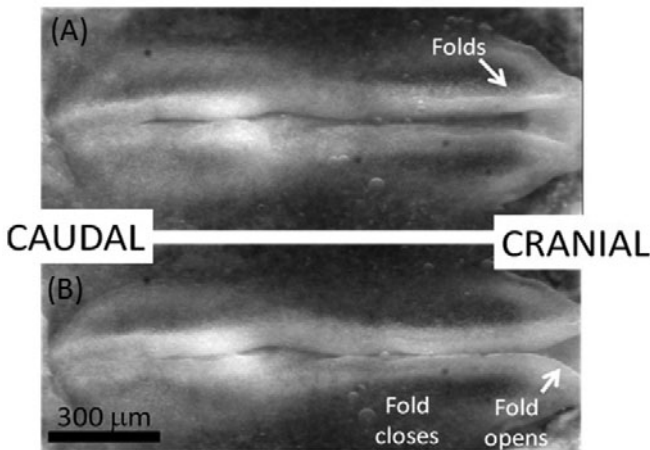


Fig. 1. Two snapshots of the neural crest at 15 minutes interval. (A) Just prior to the collision, the folds are parallel to the Antero-Posterior axis, and make a U-turn in the head area. (B) Just after the collision, the folds have merged in the central area, but in the head area they move asunder instead of merging, and the folds fan in a T shape (white arrow).

occurs otherwise, by cavitation of a thick neural chord [16]. The case of fish will be discussed in the conclusion together with the cephalochordates.

The 2D flow of the ectoderm folds, and the way they roll up in chicken (so-called primary neurulation) was not so far analyzed in full quantitative detail. The first purpose of this article is to extract and interpret the vector fields of movement at a quantitative level, a second purpose is possibly to infer how such a mechanism of formation may have appeared.

In order to address quantitatively the movements, we performed a careful observation of the formation of the presumptive head rudiment in chicken embryos (fig. 1, Movie 1). Current technical tools, associated to our special sample preparation, allow one to follow continuously the entire vector field of morphogenesis in the chicken embryo, especially at early stages, when the embryo is almost flat and not too dense optically.

The rudiment of head first appears (in a day-2 chicken embryo) as a T-shaped fold located at the apex of two parallel folds forming the dorsal backbone (“neural plate”). As they roll up, these folds come into contact and form the neural tube. Time-lapse microscopy of these embryo folds shows that the T-shaped form of the head rudiments, including the formation of the eye cups, where eyes develop, is a mere consequence of the collision of the left and right lips of the folds.

In physical, mechanistic, terms, the tissue flow is, first, dipolar, as it progresses towards the midline (median axis of the embryo). By dipolar, it is meant that the flow of each half of the embryo, towards the median axis, can be understood on the basis of classical hydrodynamic approach, in which directional flows are imposed oriented in one direction. Monopolar flows are flows with a punctual source or sink of flow. Dipolar flows are conservative flows, with a localized forward impulse, as for example in vor-

tex rings [17]. The form of the flow (its kinetics) is driven by the conservation of flux in space ($\text{div}(V(x, y)) = 0$), while the dynamics of the flow is driven by Newton’s law. Inertial flows may be conservative in space and time. In case of viscous dissipation, the flow decays, and although conservative in space, the flow is non-conservative in time. However, if a constant force is exerted, a constant viscous dipole may be generated [18]. A constant cellular traction provides such a constant force for embryonic movement.

In 2D hydrodynamics, the formal analogy between magnetic dipoles and hydrodynamic dipoles stems from the spatial conservation law for the flux. The fact that slow creeping flow dynamics may apply to embryonic tissue stems from the fact that thin incompressible visco-elastic shells behave like a Poiseuille flow in the long term [18] (assuming that early embryonic tissue, which is 90% water, is incompressible).

While the tissue of each half flows towards the median axis and invaginates, each half behaves as a spatially independent flow, and the force at the boundary creates a situation of a dipolar flow oriented towards the median axis. However, as the left and right halves of the embryo meet, a collision of the two dipolar flows occurs. After this collision, the flow in the entire field is the superposition of the dipolar flows on either halves, and is thus quadrupolar. We expect the superposition to be linear, since the flow is extremely slow ($\sim 1 \mu\text{m}/\text{min}$) in a very small mass of size $\sim 1 \text{mm}$.

During the entire process, the data show that the bulk flow is mathematically continuous, and even constant. The only discontinuity which we observe is a physical discontinuity associated to the collision of the left and right halves of the embryo, along the boundary condition at the median axis. This boundary condition along the median axis is either a free boundary condition prior to the collision of the two halves of the embryo (fig. 2(A)), because the sheets invaginate underneath instead of touching each other, or a reflection condition (fig. 2(B)), when the two halves of the embryo have met. As a consequence, there is, indeed, a discontinuity in morphogenesis which explains the early formation of the head parts, but it is a geometrical, dynamical, one.

The discontinuity is observed in the entire morphogenetic field, and it happens by the minute, at the moment of the collision. This can only be explained by a mechanical propagation of the morphogenetic forces, diffusion being unable to smoothen and propagate a morphogenetic gradient so rapidly.

In order to confirm this result by independent measurements, we have measured by air puff tonometry [19] the visco-elastic time constant of the embryonic tissue, and the data confirm a simple visco-elastic behaviour, with a visco-elastic element in series with a viscous element.

Materials and methods

Chicken embryos were incubated in a standard Minitüb incubator, maintained at 38°C . The embryos were filmed through a glass window with a B&W Watek 512 analog

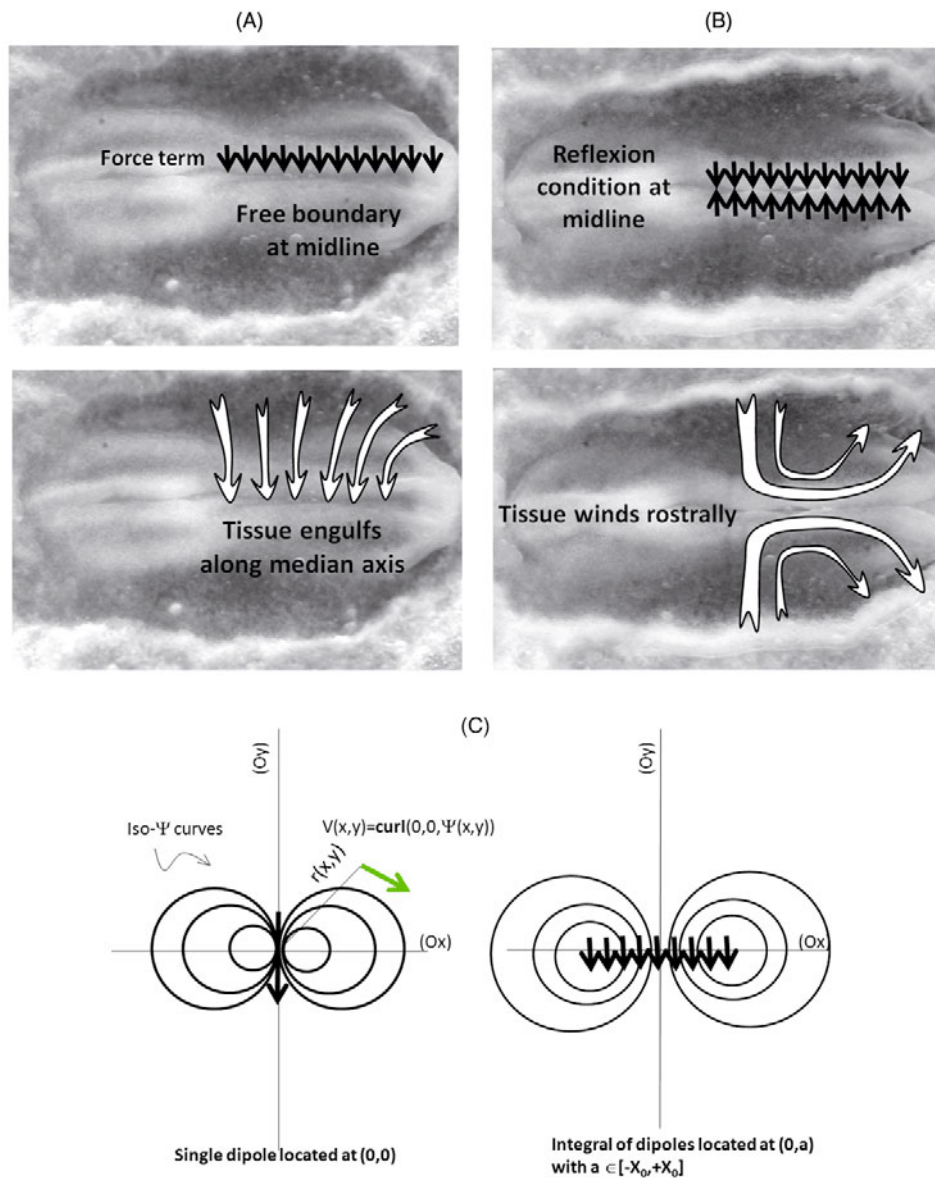


Fig. 2. Schematic physical interpretation of the situation prior to the collision of the folds of the right and left parts of the embryo (A), and just after the collision of the folds (B). In (C), the flow field is found by the stream function technique, by integrating the field generated by single dipolar force terms located along the edge that pulls the ectoderm forward. In this image we show the heuristic for the calculations: first assume a single pulling force. This is mathematically a dipole located at one given point (a, b) (here: $(0,0)$). Then integrate the displacement map of all forces along the pulling edge, assuming the pulling edge is located on the segment of points aligned between $x = -X_0$, and $x = X_0$, at coordinate $y = Y_0$.

camera interfaced with the Scion Image software adapted from Wayne Rasband's NIH Image. In order to get better images, the embryos were entirely removed from the shell, and the yolk was carefully rinsed away. The embryo was then placed in a Petri dish in PBS buffer with additional fetal-calf serum. Embryos could be cultured this way for up to 3 hours, prior to showing signs of starvation. The analyses shown below are performed during 140 important minutes of normal development, when the neural folds are just folding and merging (or not merging, see below), in the rostral area (rostral area = anterior area,

in the future chest and head region). The supplementary data film (Movie 1) spans 50 minutes before, and 120 minutes after, the merger of the left and right halves. This event is filmed here with a time resolution of 1 minute. The tissue velocity was assessed by Particle Imaging Velocimetry (PIV tracker module courtesy of B. Abou and O. Cardoso, available upon request). The supplementary film presented here was obtained at magnification $\times 4$ on a Leica MZFLIII binocular microscope.

The air puff tonometry data were acquired using a newly developed instrument [19]. Except that, in the ver-

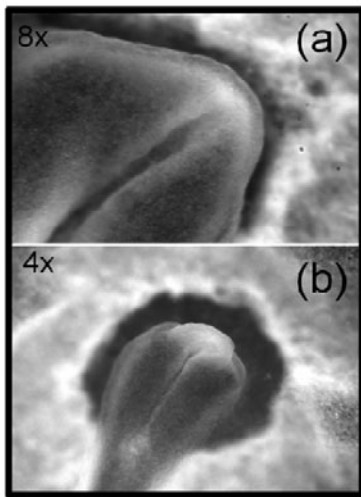


Fig. 3. (a) Shape of the folds, prior to the collision of the lips of the folds, and (b) 2 hours after. The T shape of the folds, in the head area (b), is formed by the change in boundary condition of the visco-elastic deformation field. As a consequence, the (future) eye cups start to evaginate sideways.

sion used here, a rapid camera Photron fastcam was used, instead of a video B&W camera. The air puff measurement consists in applying a shot of air of 4 mbar (corresponding to a flow of 7 cc through a pipette of diameter 100 micrometers), and measuring the time response of the surface. The head of the embryo is positioned ahead of the tip. The light is oriented very close to specular reflection. When the air puff occurs, the head is flattened by the air shot, and the specular reflection appears bright over a shadow background (shadowgraphic image). We measure the diameter of the flattened area during time. The time transient gives the visco-elastic time scale of the tissue, the asymptotic deformation rate gives the viscous behaviour.

Experimental results

The observation reveals two phases during the formation of the neural plates (fig. 1). First, one witnesses the formation of an elongated fold along the Antero-Posterior (A-P) axis (fig. 1(A), fig. 2(A), fig. 3(a)). This occurs as the tissue moves *towards* the A-P axis (fig. 3(a)). Since the embryo has a finite size, the edges of the folds make a U-turn at the very apex of the embryo median axis, in the (future) cranial area (fig. 3(a)). The folds, which will eventually form the dorsal area, are advected towards the median axis at a constant speed in time, with a slightly spatial dipolar curl oriented head-bound (fig. 4(A), arrows pointing towards the cranial region). Why the tissue is advected is an important question which I discuss later in this paper.

The observed velocity field is constant in time: obviously the gap between the two folds closes down at a constant speed (fig. 5(A)). Therefore, the two halves of the embryo get progressively closer, until they touch each other and form the dorsal area. A true collision occurs

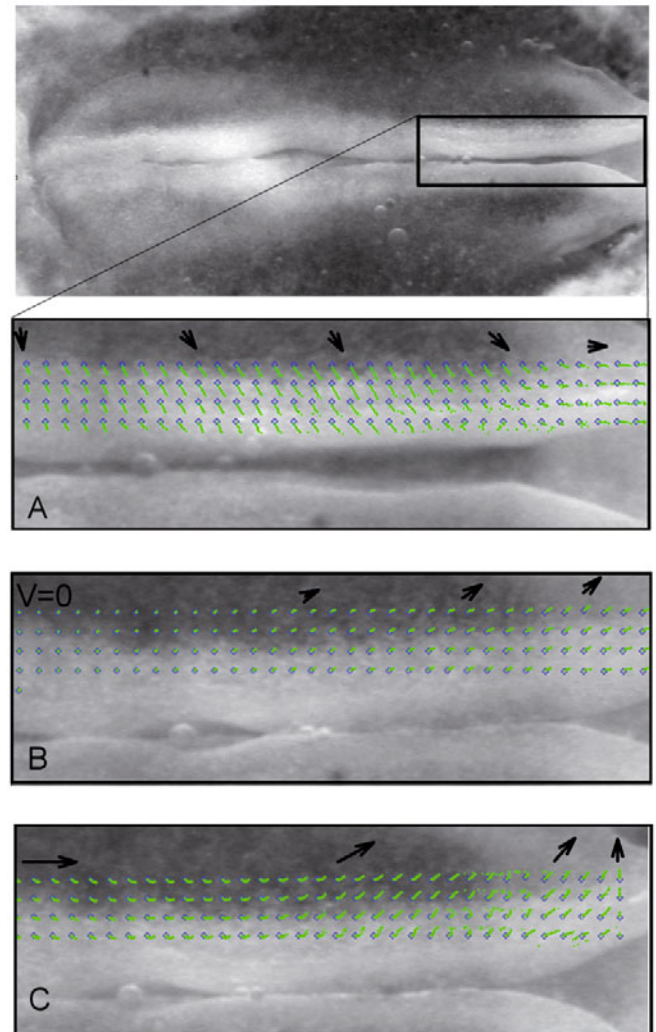


Fig. 4. (A) PIV tracking across the Movie 1. 10 minutes prior to the collision, the flow is oriented towards the midline, with however a small dipolar curl oriented towards the anterior region. Right in the anterior region, (to the right) the flow is oriented parallel to the median axis. The cranial fold has no reason to expand laterally. (B) 10 minutes after the collision, the velocity is simply zero in the area of the presumptive navel, and the tissue has no other means than growing more forward, in a quadrupolar fashion (*i.e.*, it is oriented towards the anterior region, with a component away from the median axis due to conservation law). The tracks represent 10 minutes of development. In the cranial area, the tissue fold starts to move away from the median axis. (C) 20 minutes of tracking, 20 minutes after the collision. The head folds move massively away from the median axis (arrows), even perpendicularly to it in the foremost area (which will be actually the eyes and nasal area). The neural folds will therefore generate a head. They will actually close much later, but in the meantime, the eye cups will have evaginated enough laterally to form the features of the forehead.

(fig. 1(B), 2(B), 3(b), 4(B)), which induces a discontinuity in tissue flow. Because of the dipolar curl of the flow, the collision occurs in the central part first, and propagates anteriorly, closing progressively the neural crest.

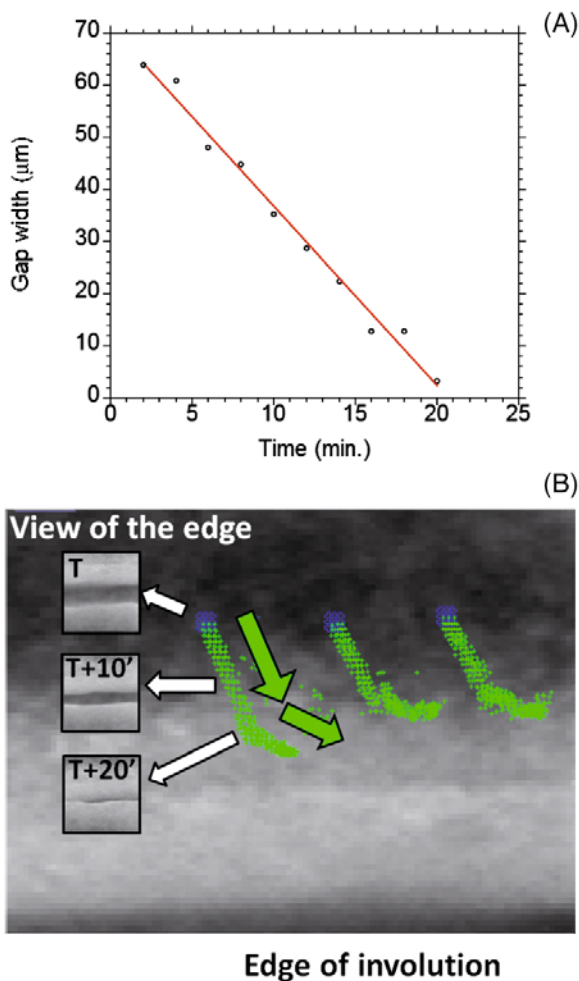


Fig. 5. (Colour on-line) (A) Following the closure of the gap in the (presumptive) navel area shows that the movement of the folds has a constant speed until the folds merge (corresponding to a gap width=0). (B) Following group of points by PIV in the presumptive navel area shows that the discontinuity of speed is directly associated to the closure of the gap. The boxes show a wide field view of the gap between the two edges of the folds, superimposed on a magnified view of the same area ($\times 4$). Blue crosses are followed in time with a time interval of 1 minute, the tracks (green) are superimposed on the first image. The boxes show the width of the gap 10 minutes ($T+10'$) and 20 minutes ($T+20'$), after the start (T) of the time-lapse tracking the blue crosses. One observes that the discontinuity in tissue speed is induced by the contact between the two halves of the embryo.

However, a more detailed analysis of the films (figs. 3, 4, 5) shows that the flow is modified by the collision in a very deterministic way. The pattern of vector field is strongly discontinuous at the moment of collision of the two folds. If we study the pattern just before the collision (10 minutes before, actually), we see that the pattern of fluid speed is oriented strongly *towards* the midline, fig. 4(A) in the central area, and more *along* the midline in the (future) cranial area. This tissue speed pattern is going to be completely modified by the mere contact of the folds.

Indeed, if we now study the vector field just after the collision (10 minutes after the collision, actually), we observe that the speed is oriented roughly *parallel* to the median axis in the central area, although with a small component oriented *away* from it in the (future) cranial area (fig. 4(B)). This evidences a change in vector field which is massive in terms of magnitude and direction, and general in terms of geographical location inside the embryo. Later (20 minutes) after the collision, the flow is oriented along the axis, in the central part of the embryo, and strongly away of it in the more rostral area, especially in the presumptive cranial area (fig. 4(C)).

In more detail (figs. 5, 6), in the area of the presumptive navel, the two lips of the left and right folds merge. Therefore, the speed falls strictly to zero there (figs. 5(A), 6(A)). In the presumptive chest area, the speed is also discontinuous, and the two lips of the left and right folds merge, but the flow, after moving towards the median line, starts to move away from the median line, although the spine is closed (fig. 6(B)). In the presumptive fore-head area (fig. 6(C)), the folds undergo a discontinuity such that the speed, which is towards the median axis prior to collision, changes sign and starts to be oriented strongly away from the median axis, and the lips of the neural crest *never* merge in the foremost part. This is to say that the collision of the lips in the “navel” area of the embryo influences dramatically the pattern of tissue movement much forward in the head area, such that the lips of the neural crest folds in the anterior part of the cephalic region never have a chance to close there, after the collision of the two halves of the embryo has occurred in the central part of the embryo.

Tonometry results

In order to strengthen the hypothesis that the tissue behaves like a viscous material, I have studied the deformability of the embryonic head, just after the two halves of the embryo have merged. (Prior to the merger, the folds are so complex that it is difficult to deform simply the surface; after the merger of the two halves, the head exhibits a rather smooth and flat area, large enough for assessment of the visco-elastic properties.) The data in fig. 7 show the time evolution of the deformation of the head, during a constant air puff. It is observed that, after a rapid visco-elastic transient, the deformation evolves at a constant rate, characterized by the constant time variation of the deformation. Although we are unable to pursue longer the air puff, a short puff of about 5 seconds is long enough to evidence that the data do not asymptote a plateau, as for an elastic solid, but a straight line with constant slope, as for a viscous material. Therefore, for strong enough forces, and times above a few seconds, the living material behaves like a viscous fluid. A short time interval of 0.2 seconds at the beginning of the measurement is invalid, due to the ramp of the air puff, before reaching the pressure setpoint.

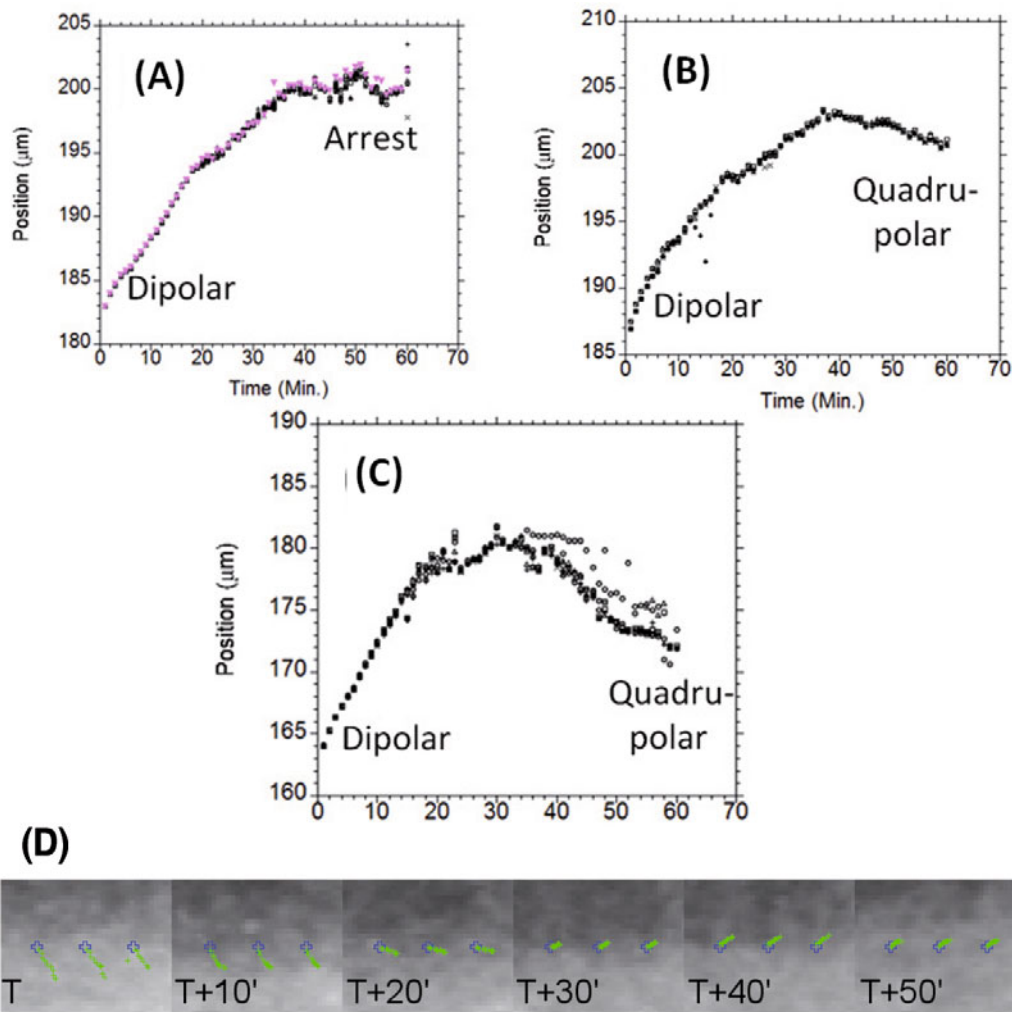


Fig. 6. Tracking of points in the time-lapse movie, through the moment of the collision. The plot represents the coordinate of the points perpendicular to the median axis. The median axis is located at position 235, in the frame. In (A), eight points located very close to each other in the area of the presumptive navel are followed. The tissue moves steadily, until it crashes against the other half, and gets arrested along the median axis. In (B) eight points are followed in a somewhat more anterior area, close to the edge of the fold. In this case, the folds move steadily, until they discontinuously move away from the median axis, although very slowly. In (C) eight points in the presumptive eye cup area show first a steady flow towards the median axis, as if the fold would simply be wrapping up uniformly, although, as soon as the folds collide in the presumptive navel area, the presumptive eye cup fold moves away from the median axis, and will therefore not close. (D) Represents the speed followed at three points located in the head area by intervals of 10 minutes, showing the rocking of the growth direction. The collision occurs between $T + 10'$ and $T + 20'$, the origin of times in (D) is not the same as in (A), (B), (C).

Origin of the flow dynamics

I now discuss the origin of the movement itself. During the collision of the two halves, and after, when it has occurred, one gets the visual impression that there exist two tissue layers, one on top, due to tissue convergence towards the median axis, and one underneath, corresponding to the same layer, but folded like a tank tread, and hence, moving away from the median axis. This is visible in the fact that thicker material has a whiter color, by light diffusion. I have filmed the further development of the head area after the completion of the collision. In such an embryo as fig. 8, the contrast of light diffusion allows one to observe very well that there exists an underneath layer of tissue parallel

to the median axis, and migrating away from the median axis. The migration speed of this layer is constant in time. The interpretation of this situation is as follows: when the buckling of the tissue starts, the fold along the neural crest behaves as a tank tread. At the area of contact of the top and bottom layers of the tread, there is a force exerted on the top layer. These observations confirm existing detailed anatomical studies of the neural tube [16] which show that the fold of the ectoderm generates layers of cells hooked “underneath” the moving ectoderm. This is classically called “apposition” of the ectoderm that forms the neural tube. Typical images found in the embryological literature are reproduced in fig. 8(D). We have taken the

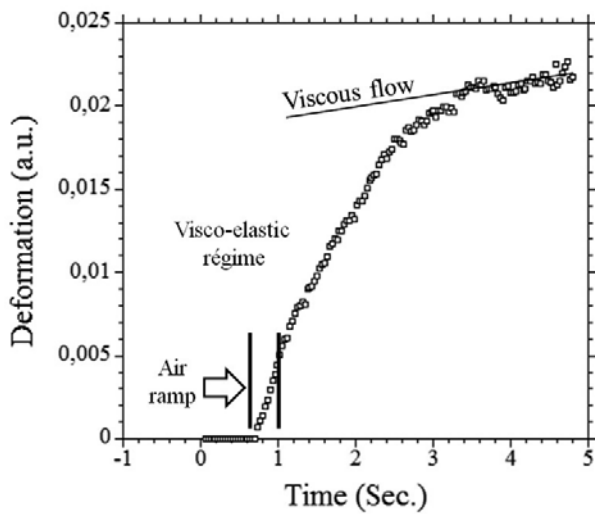


Fig. 7. Direct *in vivo* assessment of the visco-elastic behaviour of the embryo head. An air puff is imparted onto the head, and the response of the tissue is recorded by a high speed camera. A simple visco-elastic response is observed (Kelvin-Voigt type) with a time constant of 3 seconds, followed by a slow creep flow in series. In this assay the air puff has a pressure of 4 mbar, and the total air flux is 7 cc through a pipette 100 micrometers in diameter.

original figure from ref. [16], and added more details to the picture to explain the 3D organization of the tank tread.

By material conservation, if the upper layer converges towards the median axis, then the underneath layer migrates away from the median axis. By the principle of action and reaction (Newton's law), the migration away from the median axis of the portion of the tread located underneath pulls upon the top (ectodermal) layer, thereby making it move in the opposite direction. Therefore, if the left-right contraction of the tissue induces a fold, as observed, then, when the fold is folded enough to form a tank tread, the top and bottom part of the tank tread will move in opposite direction, if they pull on each other, with no vertical mixing. This question is very active in biology, and the mechanism by which apposed cell layers do not mix while they crawl on each other is only starting to be understood (in ref. [20], one finds an interesting analysis of the way mesoderm crawls underneath ectoderm, which is basically the sort of mechanism needed for the model presented here). If we admit that the cell layers do not mix, as they fold, we understand that the tissue finds itself in a composite state formed of a sandwich of layers exerting opposite forces, and moving in opposite directions. Prior to closure of the folds, the tank tread forms a narrow layer along the neural crest, such that we may expect the force causing the viscous drag to have, in a first approximation, the form of a narrow rectangle located along the neural crest, with the long axis parallel to the Antero-Posterior axis.

Mathematical and physical modeling

I now proceed to demonstrate mathematically that the change in flow direction is due to the mere contact of the two lips of the folds.

In order to do so, we proceed as follows. Following ref. [21], which is confirmed by the previous observations, I assume that the flow of the tissue progresses towards the midline with a force term located in the area of the fold, and perpendicular to the Antero-Posterior side of the fold (a recent modeling of *Drosophila* gastrulation gives an interesting instance related to this one, from a physical point of view, although it is not the same animal model [22]). Please note that the pulling segment is geometrically oriented parallel to the Antero-Posterior direction, but that the direction of pull of the cells inside this segment is perpendicular to the A-P direction. This is due to cells crawling underneath on the thin film, and pulling it. Figure 8 shows that the pulling line is roughly parallel to the A-P axis. The force term is therefore composed of cells orthogonal to that line, but stacked parallel to that line.

The dipolar flow of a thin viscous material dragged by a single moving cell [18] along a surface can be written $\mathbf{V}(x, y) = \alpha \text{curl}(0, 0, \Psi(x, y)) = \alpha(\partial_y \Psi(x, y), -\partial_x \Psi(x, y), 0)$, where $\Psi(x, y)$ is the stream function with respect to a dipole located at (a, b) , and α a dimensioning prefactor proportional to the magnitude of the pulling force, $(0, 0, \Psi(x, y))$ is the vector-potential of the flow.

For a dipole of force of magnitude 1 located at coordinates (a, b) , the mathematical expression of $\Psi(x, y)$ in the entire mathematical plane of the flow is

$$\Psi(x, y) = \frac{x - a}{(x - a)^2 + (y - b)^2}. \quad (1)$$

The streamlines are circles tangent to the force. The magnitude of the coordinates of the speed will read

$$V_x(x, y) = -2\alpha \frac{(x - a)(y - b)}{((x - a)^2 + (y - b)^2)^2}, \quad (2a)$$

$$V_y(x, y) = -\alpha \left[\frac{1}{(x - a)^2 + (y - b)^2} - \frac{2(x - a)^2}{((x - a)^2 + (y - b)^2)^2} \right], \quad (2b)$$

where α is a dimensioning prefactor proportional to force traction. It is necessary to pass through the stream function in order to calculate the speed, especially when considering other distributions of forces. These will be obtained by calculating the integral of the stream function, and then the speed components by the curl of it. For an elongated horizontal segment (as in fig. 2) limited by $X = X_0$ and $X = -X_0$, having at time t a position $Y = b$, the flow map, assuming a steady state, can be obtained by a mathematical integral over the spatial variable ψ of the stream function for a single dipole

$$\mathbf{V}(x, y) = \alpha \text{curl} \left[0, 0, \int_{-X_0}^{+X_0} \frac{x - a}{(x - a)^2 + (y - b)^2} da \right]. \quad (3)$$

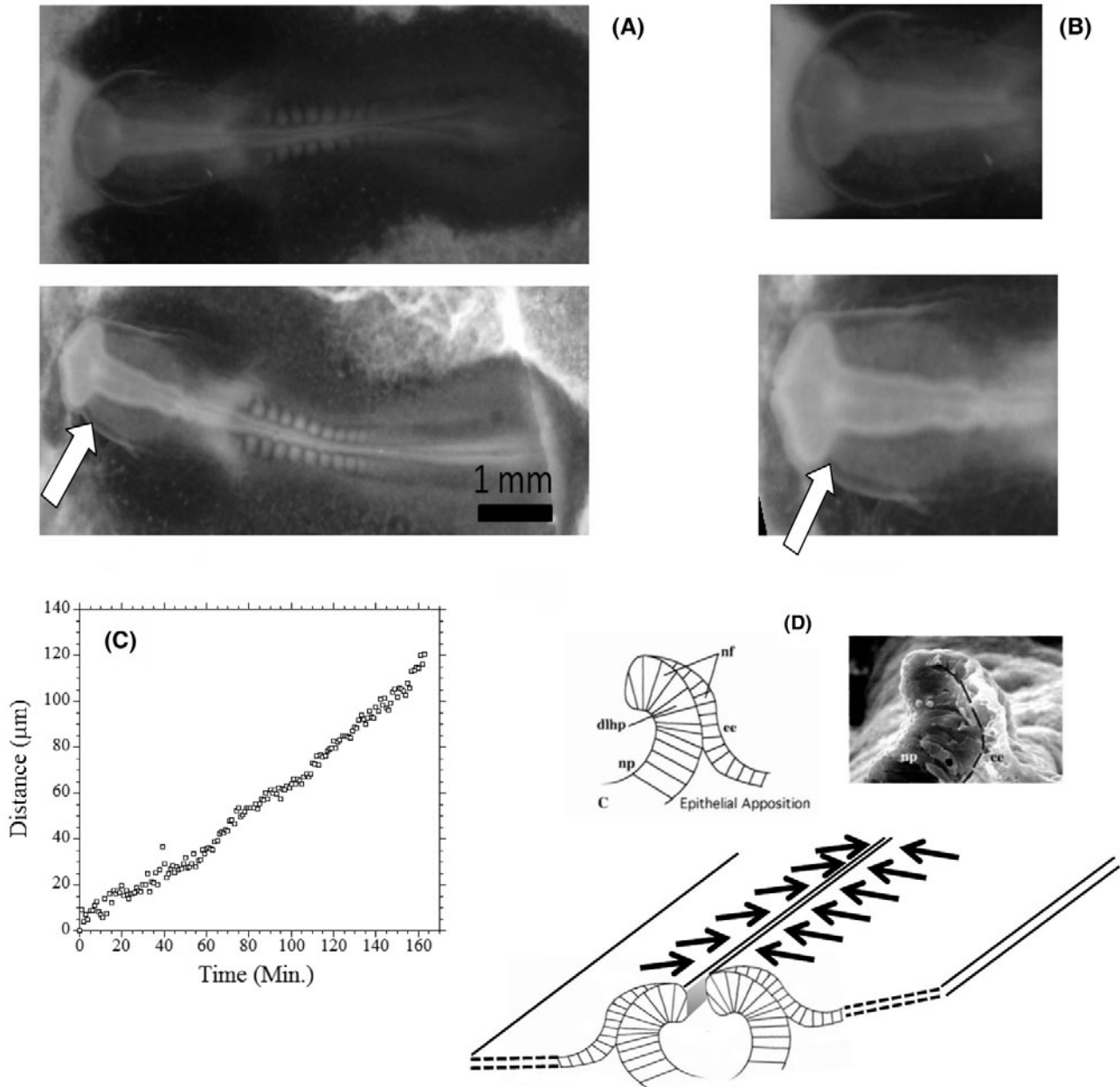


Fig. 8. Typical embryos, 4 and 6 hours after closure of the median axis. (A) The entire embryos. (B) Magnifications of the head area. One observes contrasts of black and white due to different optical densities of the tissue. The increased optical density (“whiter”) in the head area, forming a region parallel to the median axis, is linked to the fact that the tissue is thicker. One observes actually an underlying layer forming an edge, which migrates from the median axis away. When this edge is followed in time, it is seen that it moves away from the median axis at a constant speed, (C). The edge eventually reaches the lateral sides of the ectoderm, where it arrests itself. At the moment of arrest, the edge of this layer is very conspicuous (forming a crisp line, arrow in (A,B) bottom). (D) Shows a scheme of the cross-section of the ectoderm, based on ref. [16], and with the force terms added. This force term is created by the drag of cells at the apposition.

This way we find

$$\Psi(x, y) = \ln[(x - X_0)^2 + (y - b)^2] - \ln[(x + X_0)^2 + (y - b)^2]. \tag{4}$$

This corresponds to the sum of two flows whose streamlines are circles located at the tips of the pulling segment.

The speed components are

$$V_x(x, y) = \frac{2\alpha(y - b)}{(x - X_0)^2 + (y - b)^2} - \frac{2\alpha(y - b)}{(x + X_0)^2 + (y - b)^2}, \tag{5a}$$

$$V_y(x, y) = -\frac{2\alpha(x - X_0)}{(x - X_0)^2 + (y - b)^2} + \frac{2\alpha(x + X_0)}{(x + X_0)^2 + (y - b)^2}. \tag{5b}$$

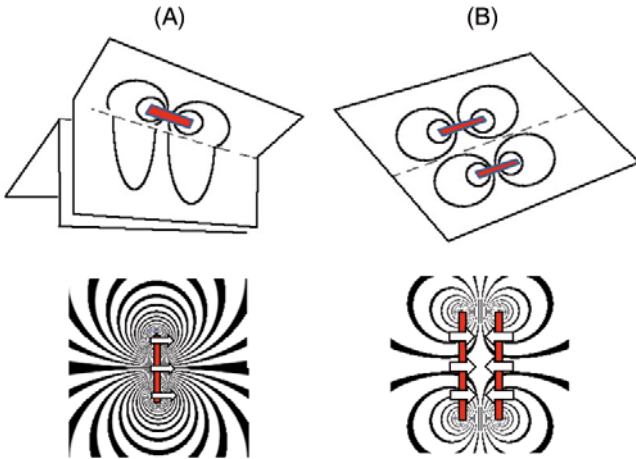


Fig. 9. (Colour on-line) During the progression of the tissue towards the median axis, the deformation rate field undergoes a change in boundary conditions. As long as the lips of the folds do not touch each other, the situation is as in (A). The plane of the tissue is folded out-of-plane, and the in-plane field runs on a free boundary along the edge. Each half behaves as a single mathematical domain, although folded. By free boundary it is meant mathematically that, if the plane is unfolded by thought, there is no specific condition on the field of speeds along the midline. Only the forces are specified there. The pulling area is indicated by the red rectangle (mind that actually, the force is exerted by the unfolded layer). The forces simply pull along the edge. The integral of the forces gives the flow shown in (A), bottom. The map in (A), bottom, simply shows the actual streamlines that would be generated by a segment (shown in red) pulling in the way indicated by the arrows. In this situation, the surface of the ectoderm is pulled forward freely, and seen from above, the entire ectoderm surface behaves as two dipolar flows running on each folded half, with a free boundary for each along the median axis. When the lips touch each other, the in-plane situation is that of two vortex dipoles with a reflection condition in the middle, this is to say, a quadrupole (B). The reflection condition is satisfied automatically when the two source terms are placed in the same mathematical domain. Therefore, the flow which is oriented towards the median axis, during the dipolar flow, falls down to zero in the central area, and curls away from the median axis more anteriorly.

This flow corresponds actually to two logarithmic vortices located at either ends of the segment. The plot of the iso-curves of the stream function (fig. 9(A)) shows it graphically. While the lines in fig. 2(C) were drawn schematically, the streamlines in fig. 9 were drawn exactly with a tabler.

We have observed that the tissue flow involutes at the fold edge along a line perpendicular to the flow (figs. 1, 2, and fig. 9(A)). Prior to collision, we have to invoke a free boundary along the median axis for the flows coming from the left and from the right. This corresponds to the flow pattern shown in fig. 9(A). We assume that the presence of the fold does not modify the in-plane cell kinetics. Now, at the moment of collision, the folds merge, such that the boundary condition along the mid-line is modified (fig. 9(B)). In such a case, one must write in the plane

the sum of the contributions of each side, so that the flow is now quadrupolar, fig. 9(B) bottom.

Therefore, at the moment of merger of the two halves, the forward flow towards the median axis (eq. (5), with $b = 0$), with its small dipolar component, jumps discontinuously to a quadrupolar flow oriented cranially and caudally, with $b \sim Y_0$, with Y_0 the radius of curvature of the fold. In this case, and considering the width of the fold lips as Y_0 , the flow will be approximated by

$$V_x(x, y) = \frac{2\alpha(y - Y_0)}{(x - X_0)^2 + (y - Y_0)^2} - \frac{2\alpha(y - Y_0)}{(x + X_0)^2 + (y - Y_0)^2} - \left[\frac{2\alpha(y + Y_0)}{(x - X_0)^2 + (y + Y_0)^2} - \frac{2\alpha(y + Y_0)}{(x + X_0)^2 + (y + Y_0)^2} \right], \quad (6a)$$

$$V_y(x, y) = -\frac{2\alpha(x - X_0)}{(x - X_0)^2 + (y - Y_0)^2} + \frac{2\alpha(x + X_0)}{(x + X_0)^2 + (y - Y_0)^2} - \left[-\frac{2\alpha(x - X_0)}{(x - X_0)^2 + (y + Y_0)^2} + \frac{2\alpha(x + X_0)}{(x + X_0)^2 + (y + Y_0)^2} \right]. \quad (6b)$$

Therefore, the change in flow due to the change in boundary conditions induces a massive discontinuity of the speed, from the form of eq. (5), to that of eq. (6). This discontinuity is characterized by a jump from a dipolar to a quadrupolar pattern. In the true embryo, this occurs in 1 minute in the central area, and with a smoother time constant in the head area.

The mathematical fact which discriminates a mechanical explanation from a chemical one is actually encapsulated in eq. (6), but it deserves a more thorough explanation.

When writing the fluid velocity in the embryo tissue as a mechanical sum of what is going on on the left and what is going on on the right (eq. (6), terms corresponding to $-Y_0$, and to $+Y_0$), it is assumed that along the contact line existing along the mid-line of the embryo, the physical forces are physically transmitted by the tissue, via the viscous drag. When solving for the entire fluid dynamics, there remains only this sum, in which this assumption is no longer apparent, although it is present. Why is such an assumption justified? By *gedanken* experiment, one can imagine that the left part of the embryo could as well be static, and that a moving visco-elastic fold would arrive from the right part. In such a case, at the moment of contact, the left part would move and be stirred by the right part anyway, regardless of its own motion, by the mere visco-elastic contact along the common edge of both parts. In small speed regimes, the speeds are additive, such that, the mechanical propagation of the vector field (which propagates at speed of sound) amounts to a mere sum of the two terms. This fact is solely the consequence of a change in boundary conditions, in an otherwise monotonous and continuous developmental speed. Stated otherwise, the right half pulls almost instantaneously the entire left half along the edge by visco-elastic shear, and vice versa, but chemical gradients cannot explain this almost instantaneous transmission of the velocity change.

Indeed, such a discontinuity, as observed in the experiment, cannot be explained by chemical diffusion in an embryo. If the change in tissue movement were induced by chemical gradients, the flows would be unchanged in the bulk of the embryo, far from the midline, at the moment of first contact of the two parts of the embryo, until chemical gradients would have smoothed and diffused away from each half, to the other half. But we observe a change in physical speeds in the entire embryo, of the order of 100% in about 1 to 2 minutes. This is to say that chemical fields of proteins would have to diffuse and stabilize by say, 2 minutes. Recent data provide diffusion constants of growth factors implied in embryo development such as FGF8 in the $50 \mu\text{m}^2 \text{s}^{-1}$ range [23]. The diffusion length for such diffusion constants is $L = \sqrt{Dt}$ which is typically $t^{1/2} \cdot 7 \mu\text{m}$, with $t = 120 \text{s}$, that gives a diffusion length of about $80 \mu\text{m}$. I do not see how chemical diffusion could be the cause of the massive change in vector field which I observe.

Now, fig. 9 explains only qualitatively what occurs at the moment of contact between the two parts of the embryo. A quantitative analysis is given in fig. 10. The first row (fig. 10(A)) shows the two lines used for comparison with theory. Figure 10(B), left, shows the components of the speed, V_x and V_y along the line in fig. 10(A), top (dipolar flow, prior to collision). V_x is the horizontal speed (the speed along the Antero-Posterior axis, with the following convention: a positive speed is towards the rostral end), and V_y the vertical speed (from the axis away, a positive speed is a speed towards the median axis). Figure 10(B), right, gives the corresponding analytical data for a fluid dipole, with a length estimated from the length of the embryo folds. We have shown the geometry on the embryo on top of the graphs. The bottom row, fig. 10(C), shows the V_x and V_y along one line of fig. 10(A), bottom, chosen such that the distance to the midline is identical in fig. 10(B), and fig. 10(C), and the same parameter is taken in the formula. The difference in the dynamical trend is completely obvious, and these curves show how massive and general the discontinuity is. Also, the curves show a clear correlation between V_x and V_y in both cases, which are clearly not independent variables. This is actually a consequence of the field equations, since the conservation law $\text{div}(\mathbf{V}(x, y)) = 0$ in two dimensions correlates V_x and V_y .

The dipolar flow (fig. 10(B)) is characterized by a large positive V_y magnitude in the central area (the tissue goes towards the axis), and a small V_x component in the central area. Going more towards the rostral area, the V_x component increases (dipolar curl of the streamlines). Now, after the collision, the speed becomes negligible in the central area, and the flow is oriented mostly towards the rostral area. The V_y component is away from the median axis (V_y negative). The difference in trend of the two components V_x , V_y when going away from the central area towards more rostral parts is very clear. This difference is reproduced by a quadrupolar flow, with, again, length and position parameters extracted from the geometry of the embryo. Of course, the model is over-simplified, in that, in the most anterior part, the tissue is quite folded. There, the boundary conditions are modified. This may

explain the lack of accuracy of the model in that area. Other sources of discrepancy are the fact that the actual embryo is bending in 3D, that we assumed a slow Stokes flow for the tissue, and that prior to collision, the edge of the embryo halves are not strictly straight. Also, the force terms may be uneven along the edge.

Nevertheless, I believe that the hydrodynamic model grasps the essence of the phenomenon. The tissue collision is a very simple phenomenon, with trivial consequences, and although the constitutive equation might be more complex, the phenomenon in itself is not. In other words: the conservation law inside the ectoderm, which is dragged along a straight line, suffices to explain the vector fields which are observed. The exact physical properties of the material are secondary.

Moreover, the flow typology looks actually simpler than the logarithmic variation which I suggest, this is to say that the flow motion seems to be even less non-linear than the minimal non-linearity which I have introduced, and that actually a simpler model, rather than a more complex one may be at play. A simplifying factor could be that by assuming a force term acting along a line, I assume too concentrated a force. A wider pulling area will induce an even smoother velocity field.

Discussion and conclusion

These observations show that the movement of collision of the two halves of the embryo can be described by a simple flow. It consists of two tank treads which are moving towards each other. The existence of this tank tread is known in embryology and called ‘‘apposition’’. It is shown here that very simple source terms along the median axis (uniform pull) suffice to reproduce the observed movements. A line of cells pulling forward the tissue towards the median axis suffices to reproduce the trends of the data, almost at a quantitative level. Despite all the approximations, the results show that the spatial components of the field velocities are not independent. The $V_x(x, y)$ and $V_y(x, y)$ components of the speed are correlated by conservation laws which imply a constraint on the morphology of the vector field. It is not trivial that such conservation laws apply. This is why such a demonstration, as presented here, was necessary. Indeed, it is generally thought in biology that cells move individually by chemotactism. In such a case, cells could as well cross each other along the median axis. The analysis of the movie presented here shows that the entire tissue behaves as a classical continuous medium, as encountered in fluid mechanics, and not as a collection of independent moving entities.

Figures 4(A) and 5(A), which show the motion of the lips of the two halves of the embryo, show that the speed is constant in time prior to collision, although not in space (it has a dipolar curl towards the head). This movement would have continued unchanged if not for the collision with the tissue ahead. *Idem*, the flow in the cranial region would have continued to close the neural folds, if not for this collision. The collision reorganizes the flow with a strong forward recirculation due to fluid conservation.

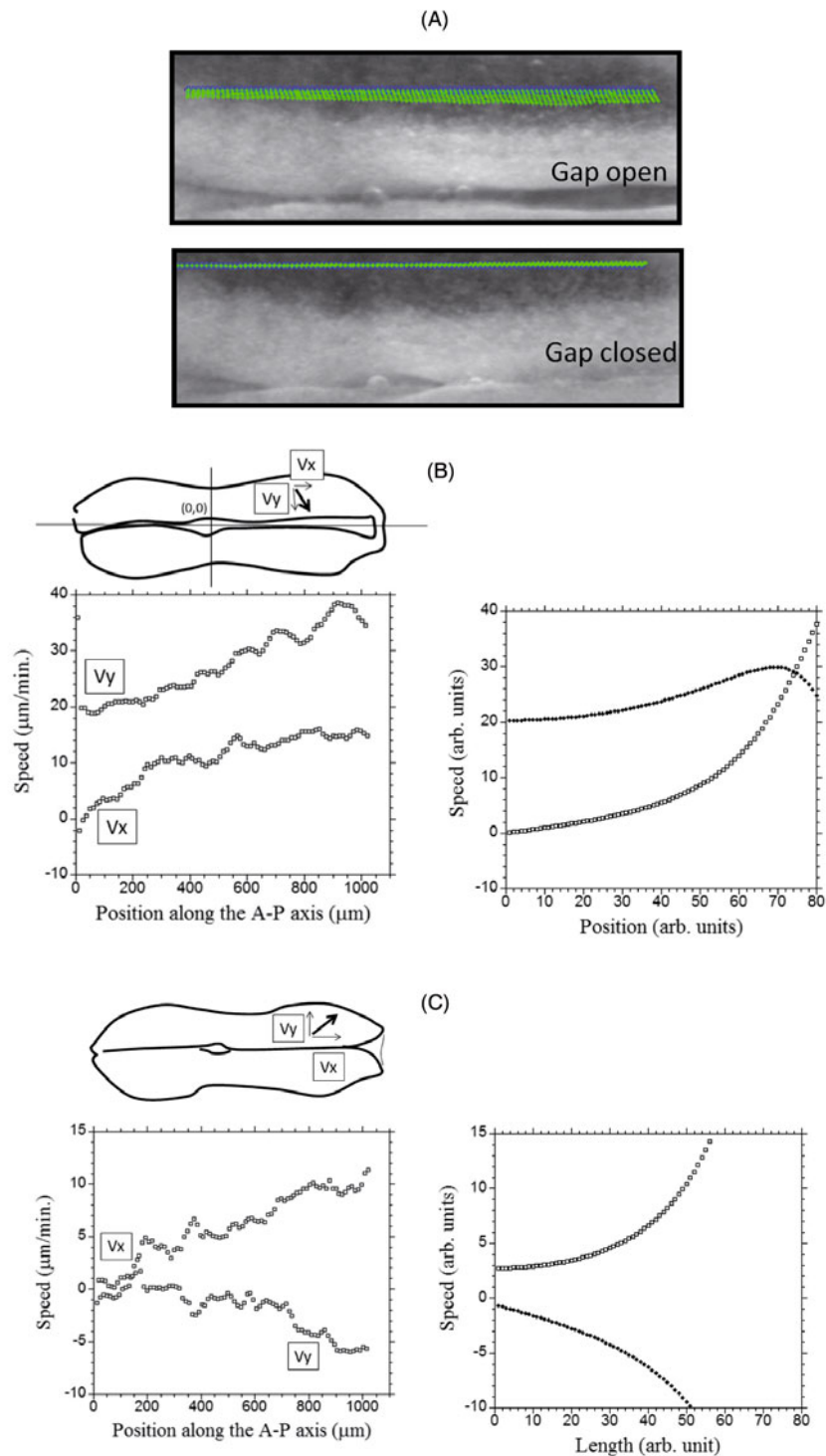


Fig. 10. (A) detail of the area where two lines are selected, prior to the collision, and after the collision (mind the gap). There is half an hour between the two. (B) Analysis of the flow prior to the collision. The dipolar flow is characterized by a progressive rotation of the vector direction from the central area, towards the rostral area. This is observed in the actual embryo, and reproduced by the equation for the dipolar flow ((B) right). The parameters are the length and position of the pulling line, and the magnitude of the pulling force simple (prefactor of the amplitude). (C) The quadrupolar flow is characterized by a negligible speed in the central area for both components, and a progressive increase of the speed *towards* the rostral area, and a negative increase, meaning an increase of the magnitude of the component of the speed, *away* from the median axis. This trend is well reproduced by the model, (C), with the same parameters, for a quadrupolar flow. Especially, the magnitude of the flow in the quadrupolar situation is much reduced as compared to the dipolar, since the forces of both halves basically cancel each other (they are oriented head-on). This last effect is quantitatively reproduced.

This forward reorientation induces a different behavior in the central part of the body, and in the anterior part. The anterior part is pushed sideways by the flow circulation, away from the median axis, and opens instead of closing, as opposed to what it does elsewhere along the A-P axis. There exists a critical point in anatomy which is the final point of the neck where the presumptive spine ceases, and the presumptive brain territory begins. This point seems to correspond to the point where the new quadrupolar component starts to overcome the remaining dipolar component, during the establishment of the contact (transient between two steady states), such that the tissue flow direction is reversed.

As observed here, the presumptive forebrain corresponds to the area which, as a consequence of a change in flow direction, has remained open after the collision (fig. 10). The eye cups correspond to the trail of the fold whose lateral evagination is induced by the Antero-Posterior reorientation, after the collision of the tissue. While the neural crest will eventually globally close, what occurs at this moment creates a lateral evagination which remains for good and will be the eyes area in the end.

One important aspect of the question addressed in this article, is that there exist gradients of orientations and magnitudes of growth speed, which visibly have nothing to do with gradients of molecules. Especially, one observes that speeds may vary spatially from zero to a maximal value V_0 , although it does not imply the existence of any chemical gradient oriented in the same direction. A mere geometrical contact and a uniform vectorial push suffices to induce such functional variations, by the laws of physics.

Moreover, the growth speeds before and after the collision are constant in time, which is quite unexpected for a process which has undergone 500 million years of random evolution. It seems that actually, the physical field controls and compels the variation of the fluid velocity.

This work raises the possibility that the origin of animal forms could be, at least in part, a dynamic phenomenon, with stochastic parameters [21]. Indeed, there exist primitive, bilateral chordates which do not have head features (no skull, no eyes, no nasal pit, they have just an oral opening). These are called cephalochordates [13]. They appeared at the Cambrian explosion, about 540 million years ago [24]. Animals with more complex head features appear later. Darwinian evolution [25] ascribes the appearance of different animal forms to selection and survival of the fittest. However, such a concept does not explain the morphogenesis at a mechanistic level, and why it is at all possible that new features will form, seemingly more complex. Genetics provides a complex insight into the morphogenesis of animals. It is, however, very rare that a direct physical, mechanistic, link can be established between genetic expressions and mesoscopic forms, like an embryonic head, which has a size of approx. 500 micrometers, at the moment of first appearance. A biomechanical study, as the one presented here, must in the end be performed, in order to complement the genetic approach, and understand the mechanical basis of tissue morphogenesis.

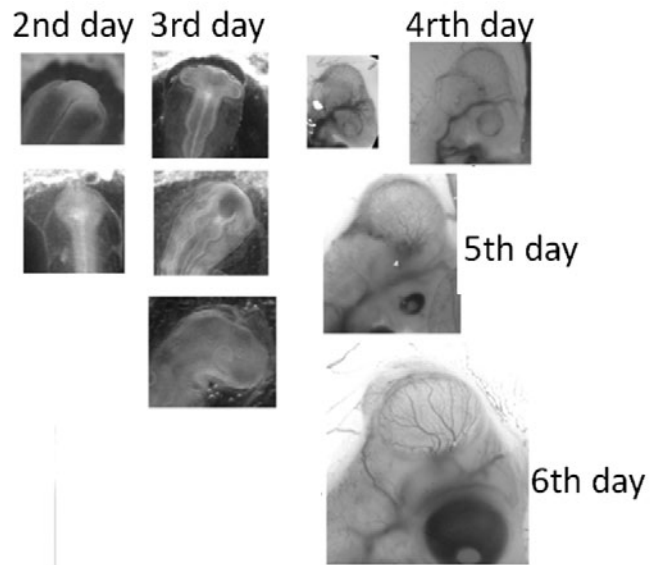


Fig. 11. Further head development in a chicken embryo, following the stage in fig. 2. Especially at the second day (2nd day bottom), the eye primordium mass is almost round, prior to a more lateral evagination (3rd day top). Animals treated with cyclopamine have a weaker neurulation movement; the eyes do not evaginate laterally, and the eye primordium is not split into two distinct masses. Thus these animals are cyclopic [27].

Analysis of animal genomes links the diversity of shapes to duplication and disappearance of entire clusters of genes (Hox genes, ref. [26]). Such stochastic mutations would explain sudden jumps in evolution, or the brutal appearance of new forms. Since genetic mutations occur stochastically, one should expect non-linear effects in morphogenesis. However, if animal parts, such as a head, were induced by non-linear feedback loops, one would naturally expect discontinuities in the morphogenetic process. The results presented here show that such discontinuities are not present, or are present as modest modulations over enormous physical discontinuities. Physically, there is no need of a jump in the developmental parameters in order to obtain such discontinuities of the morphogenetic process. In the area of the folds which form the animal body, the speed is monotonous and almost constant, with a dipolar pattern until the crash, and monotonous quadrupolar after. However, a discontinuity of the dynamics of morphogenesis is observed, which is uniquely due to the physics of the problem. This suggests that genetics controls the evolution of the head area by modifying the magnitude of the prefactors of the generic vector field, and that a more complex head lies simply “ahead” of a simple tubular head, by just pushing forward the vector field.

Interestingly enough, if the lateral evagination of the tissue forming the eye cups is weaker, as for example in embryos treated with cyclopamine [27], the embryos will exhibit a single eye located at the median axis (cyclopia). It makes sense that if the dynamics of the tissue is weaker, the lateral evagination (trail of the tissue) is weaker, and the so-called “eye primordium” is not split into two dis-

tinct masses but forms a rounder mass. Such a round mass of the eyes area is transiently observed at day 2 of a chicken development, prior to a more lateral expansion (fig. 8(B) and fig. 11). Interestingly, the single “eye spot” of the cephalochordates is also a central spot located anterior to their “brain” area.

However, not all animals neurulate exactly as was described here. Among vertebrates, there exist two types of neurulation: most animals form their neural and head parts by the folding and rolling up of the ectoderm as in the chicken. This is called primary neurulation [16]. This is how the “neural tube” generally forms. Still, in fish, the neural tube forms from a thick neurochord which hollows out [16]. Actually, this mechanism exists also in amniotes, in their tail. Therefore, the physics which was discussed here deals directly only with animals forming heads by the “neural roll up” mechanism. A more detailed study would be required, to expand the model to neural chords. Indeed, the lumen (cavity) of the neural tube is internal to the tube, but the dynamics of cellular sheets which was discussed above might not depend on whether the neural tube is full or empty, obtained by cavitation or by rolling up, since the neural tube is formed by the collision of the ectoderm edges also, albeit not completely rolled up. Two obvious caveats are, first, that fish do not have an expanded skull like birds or mammals, and, second, that birds and mammals do not have a head in the tail. Why the fish or caudal folds do not neurulate by a roll up mechanism may be related to the buckling properties of the sheet, or to the chemistry of ectoderm apposition, or to both. This question will deserve a deeper analysis of “secondary” neurulation.

References

1. J. Holtfreter, *J. Exp. Zoology* **95**, 171 (1944).
2. H.M. Phillips, *Amer. Zool.* **18**, 81 (1978).
3. D.E. Ingberg, *Int. J. Dev. Biol.* **50**, 255 (2006).
4. J.C. Gerhardt, M. Danilchik, T. Doniach, S. Roberts, B. Rowning, R. Stewart, *Development* **107**, 37 (1989).
5. W. Wilson, N.J.B. Driessen, R.C.C. van Donkelaar, K. Ito, *OsteoArthritis and Cartilage* **14**, 1196 (2006).
6. V. Fleury, *Phys. Rev. E* **61**, 4156 (2000).
7. E. Farge, *Curr. Biol.* **13**, 1365 (2003).
8. M. Unbekandt, P.M. Del Moral, F. Sala, S. Bellusci, D. Warburton, V. Fleury, *Mech. Dev.* **125**, 314 (2008).
9. A.E.X. Brown, D.E. Discher, *Curr. Biol.* **19**, R781 (2009).
10. M. Chuai, C. Weijer, *Hum. Front. Sci. Program J* **3**, 71 (2009).
11. E.A. Zamir, B.J. Rongish, C.D. Little, *PLoS Biol.* **6**, e247 (2008).
12. P. Friedl, K. Wolf, *J. Cell. Biol.* **188**, 11 (2009).
13. A.S. Romer, R.S. Parsons, *The Vertebrate Body* (Saunders College Pub., Philadelphia, 1986).
14. M. Callebaut, E. Van Nueten, H. Bortier, F. Harrisson, *J. Morphol.* **255**, 315 (2003).
15. R. Wetzel, *Vehr. physik.-med. Ges. Würzburg* **40**, H.5 (1924).
16. R. Ladher, G.C. Schoenwolf, *Making a Neural Tube, Developmental Neurobiology*, edited by M. Jacobson, M.S. Rao (Springer, Berlin, 2004).
17. K. Shariff, A.A. Leonard, *Annu. Rev. Fluid. Mech.* **24**, 235 (1992).
18. V. Fleury, *Organogenesis* **2**, 1 (2005).
19. V. Fleury, O.P. Boryskina, A.J.M. Cornelissen, T.-H. Nguyen, M. Unbekandt, L. Leroy, G. Baffet, F. le Noble, O. Sire, E. Lahaye, V. Burgaud, *Phys. Rev. E* **81**, 021920 (2010).
20. N. Rohani, L. Canty, O. Luu, F. Fagotto, R. Winklbauer, *PLoS Biol.* **9**, e1000597 (2011) doi:10.1371/journal.pbio.1000597.
21. V. Fleury, *Eur. Phys. J., A.P.* **45**, 30101 (2009).
22. P.A. Pouille, E. Farge, *Phys. Biol.* **5**, 15005 (2008).
23. S.R. Yu, M. Burkhardt, M. Nowak, J. Ries, Z. Petrusek, S. Scholpp, P. Schwille, M. Brand, *Nature* **461**, 533 (2009).
24. S.C. Morris, *The Crucible of Creation: The Burgess Shale and the Rise of Animals* (Oxford University Press, New York, 1998).
25. C. Darwin, *On the origin of Species by means of natural selection or the preservation of favoured races in the struggle for life* (1859).
26. K. Schugart, C. Kappen, F.H. Ruddle, *Proc. Natl. Acad. Sci. U.S.A.* **86**, 7067 (1989).
27. F. Marlow, F. Zwartkruis, J. Malicki, S.C.F. Neuhauss, L. Abbas, M. Weaver, W. Driever, L. Solnica-Krezel, *Dev. Biol.* **203**, 382 (1998).